J. Phys.: Condens. Matter **21** (2009) 084207 (14pp) doi:10.1088/0953-8984/21/8/084207

Materials modeling by design: applications to amorphous solids

Parthapratim Biswas[1], D N Tafen[2], F Inam[3], Bin Cai[3] and D A Drabold[3,4]

[1] Department of Physics and Astronomy, University of Southern Mississippi, Hattiesburg, MS 39406, USA
[2] Department of Physics, West Virginia University, Morgantown, WV 26506, USA
[3] Clare Hall, Herschel Road, Cambridge CB3 9AL, UK

E-mail: partha.biswas@usm.edu, DeNyago.Tafen@mail.wvu.edu and drabold@ohio.edu

Received 24 July 2008
Published 30 January 2009
Online at stacks.iop.org/JPhysCM/21/084207

Abstract

In this paper, we review a host of methods used to model amorphous materials. We particularly describe methods which impose constraints on the models to ensure that the final model meets *a priori* requirements (on structure, topology, chemical order, etc). In particular, we review work based on quench from the melt simulations, the 'decorate and relax' method, which is shown to be a reliable scheme for forming models of certain binary glasses. A 'building block' approach is also suggested and yields a pleading model for $GeSe_{1.5}$. We also report on the nature of vulcanization in an Se network cross-linked by As, and indicate how introducing H into an a-Si network develops into a-Si:H. We also discuss explicitly constrained methods including reverse Monte Carlo (RMC) and a novel method called 'Experimentally Constrained Molecular Relaxation'. The latter merges the power of *ab initio* simulation with the ability to impose external information associated with RMC.

(Some figures in this article are in colour only in the electronic version)

1. Introduction

Amorphous materials and glasses continue to play an important role in technology, with applications ranging from photovoltaics to fiber optics and fast-ion conducting glasses showing promise for low power non-volatile computer memory applications. The amorphous state itself poses some of the most basic questions in solid state physics: the nature of the glass transition, the origin of anomalies in the low temperature specific heat, the nature of electronic and vibrational states in a topologically disordered network and many more beside. A question of considerable current interest is the topology and nanoscale ordering of the 'intermediate phase' of Boolchand [1].

For modeling glasses 'by design' it is natural to incorporate *a priori* information about the material in some form. We refer to this as a 'biased' method below (it is biased in the sense that the procedure amounts to the external imposition of some connectivity, local chemistry, etc). We also present relevant unbiased methods that are useful in obtaining glasses with particular requirements 'by design', though to obtain the desired properties multiple runs may be necessary.

For many of these questions, the necessary starting point is an atomistic model of the material. In virtually all cases, periodic boundary conditions are used to represent bulk amorphous phases; slab models (periodic in 2D) are used for modeling surfaces [2, 3]. The modeling requirements for disordered materials amount to a perfect storm: (1) large models are required to ensure no overlap between atoms and their images in adjacent cells, to provide an adequate sampling of the range of disorder available to the material. For some problems, such as studies of electron states near the mobility edge, thousands of atoms are desirable; (2) accurate interatomic forces are required for simulations. This has been confirmed in many detailed studies, but it is almost obvious. After all, interatomic potentials are usually obtained by fitting to a limited database, often of ordered phases. Amorphous materials by their very nature manifest a broad range of local structures that poses a challenge to even the best empirical

[4] Permanent address: Department of Physics and Astronomy, Ohio University, Athens, OH 45701, USA.

potentials; (3) for questions associated with atomic dynamics, long MD simulations are needed to get adequate estimates of vibrational spectra (short simulations provide poorly resolved densities of state); (4) for the most pressing technological issues of electronic and optical behavior, one sometimes even needs accurate approximations for excited states—which is not easy even for a small system!

Methods to create structural computer models of amorphous materials fall into two categories.

Direct methods: the use of an interatomic potential (either empirical or *ab initio*) to perform an MD, Monte Carlo (or variant) simulation to find a non-crystalline conformation that is a local minimum of the energy functional. If the resulting structure compares favorably with experiment, it is accepted to be representative of the structure.

Inverse methods: the use of experimental information to build a model consistent with measurements. Typically these studies use data from x-ray or neutron diffraction, though other data and even external constraints can be applied. These methods usually are labeled 'reverse Monte Carlo' (RMC) methods [4]. They are very easy to implement and do not require any interaction potential.

The direct methods have the advantage that they are entirely unbiased—the researcher is not building in any *a priori* expectations, imposing a particular microstructure, etc. Thus, if such a calculation produces a model consistent with experiment, it is likely that the structures present in the model echo features of the real material. The direct method has the disadvantage that it often fails quite spectacularly in producing experimentally credible models. The most obvious approach is to simulate a liquid phase of the desired stoichiometry and 'quench' it on the computer, by using some form of dissipative dynamics. With some irreverence, we name this 'cook and quench'. Our experience is that such a scheme is valuable for systems in which the local ordering of the liquid phase is essentially similar to the amorphous phase (SiO_2 [5] and $GeSe_2$ [6] are good examples). For the archetypal amorphous solid, a-Si, the method fails badly in part because the liquid is a sixfold metal [7], which is very different from the highly tetrahedral amorphous phase. It is worth noting too that a-Si is not a glass, in the sense that it cannot be obtained experimentally by a melt quench method, whereas SiO_2 and $GeSe_2$ are classic glass formers. We have also found that complex glasses like $GeSe_3$:Ag are remarkably well modeled with the 'cook and quench' scheme [8].

The indirect methods hold the advantage that, by construction, they agree with whatever experiments are included as constraints. Since a really satisfactory model of any material must be consistent with all experiments on the system that we believe, this is a real virtue. On the other hand, experiments like neutron diffraction should be viewed somewhat as a 'sum rule'—the theory must agree with the diffraction data, but it is obviously impossible to uniquely invert the scattering data to obtain a structure. The trouble is that there is a tincture of information in the smooth structure factors; and this data minimally constrains the topology of a model. This is in contrast with protein crystallography, in which case there is a forest of delta functions [9]. In this case, the information content (as one could estimate from information entropy [10]) is vastly higher than for the smooth data for a glass. The RMC method [4] has been heavily employed, sometimes augmenting the experimental data with external constraints (for example, to enforce the desired coordination or chemical order).

Both the direct and indirect methods have important advantages and problems. It is therefore worthwhile to explore their validity, and particularly to try to unify the two approaches in a form more powerful than either in isolation. In addition, we will also present some other novel modeling schemes that are very useful for particular materials. The primary focus of this paper is to discuss novel methods to model glassy and amorphous materials, with particular emphasis on semiconducting glasses, using both direct and indirect methods including the 'inverse' methods. We will have little to say about cook and quench methods in this paper, as these are extensively discussed in the literature [11–13].

The rest of this paper is organized as follows. In section 2, we briefly mention the merits and demerits of direct methods ranging from empirical and semi-empirical to first-principles density functional approaches. This is followed by a discussion on emerging direct molecular dynamics approaches that attempt to include *a priori* information about the local structure and bonding environment in the simulation. In section 4, we discuss a constrained form of RMC as an illustration of a 'reverse' method, and in section 5, discuss a marriage of RMC with the use of an *ab initio* interatomic interaction. A discussion on 'polymerization' in the As–Se glassy system is then presented in section 6. Finally, in section 7, we briefly discuss first-principles modeling hydrogenated amorphous silicon, with particular emphasis on hydrogen microstructure in relation to nuclear magnetic resonance (NMR) experiments.

2. Direct methods: an overview

One of the key choices needed for simulation of a disordered system is that of the interaction potential. Accurate *ab initio* interactions are vastly more computationally expensive, but are far more reliable, especially in uncharted topologies. The choice is thus dictated by the question under consideration and the complexity of the energetics of the amorphous material being modeled.

Empirical potentials have been devised for a limited number of systems, mostly elemental. Thus, reasonable interactions exist for carbon, silicon and many metals. A handful of potentials are available for binary systems such as GeSe and SiO. To test these potentials, it is usual to compare accurate calculations from phase diagrams (giving the energy as a function of density for many crystalline phases, some hypothetical) obtained from accurate calculations. More stringent tests are possible, usually associated with forces or the phonon. Many such simulations have been reported: possibly the most thorough are the simulations of a-SiO_2 due to Kob and coworkers [14].

Practical *ab initio* simulation usually refers to a density functional approach in which the electronic density function

$\rho(\mathbf{r})$ is the basic variable rather than the many-electron wavefunction. For a given atomic configuration, an intricate mean field theory for the electrons is solved self-consistently, as prescribed by Kohn and Sham [15]. The result is an estimate of the electronic ground state energy. After computing 'Kohn–Sham orbitals' from an effective time-independent Schrödinger equation, the density matrix is easily obtained and any ground state properties are readily computed. The nonlinear nature of the Kohn–Sham equation means that this process must be self-consistently iterated to convergence. These methods are reliable for systems that are weakly correlated and reasonably small in size. Even in the limited context of *ab initio* methods, a choice must be made for efficient local orbital methods with potentially rather inflexible basis sets or plane wave methods with essentially complete basis sets, which are far more expensive for large systems. Asymptotically (for large numbers of electrons, n), all *ab initio* methods scale as n^3 or worse, unless order-n methods are used. The latter exploit a local implementation of quantum mechanics using either Wannier functions or a truncated density matrix. These are frankly tricky for disordered systems as we discuss here, and such methods are impractical in metallic systems since the density matrix then decays as a power law. An advantage of all *ab initio* methods is that they automatically provide some electronic information, though only the ground state can be discussed with rigor. From a practical point of view, many picosecond simulations are easily carried out on systems with several hundred atoms for local basis methods, and a few hundred atoms seem to be the current limit for plane wave methods. An authoritative review of these topics is available in the books by Martin [15] and Finnis [16].

The so-called 'tight-binding' molecular dynamics provides a compromise between the first-principles density functional and empirical approaches at an intermediate level of complexity. The idea here is to form an empirical tight-binding Hamiltonian, and use it to compute total energies and forces. These calculations range from fairly sophisticated approaches with explicit local orbitals and a serious attempt to approximate the Kohn–Sham orbitals to two-center Hamiltonians of an entirely empirical nature (no explicit basis functions, only rules for computing matrix elements for a given set of coordinates). This approach makes it relatively simple to obtain the Hamiltonian (and, in non-orthogonal representations, overlap) matrix, but the next step is still a matrix diagonalization, or some other scheme to avoid direct diagonalization.

In summary, it is probably good advice to study a new material with *ab initio* methods at least until a detailed knowledge of the topology and energetics of the network is available. Then it may become possible to build an adequate empirical potential or tight-binding Hamiltonian that 'mimics' the essential behavior of the *ab initio* interactions. This is usually harder than it sounds, and for most purposes we find it advisable to work with *ab initio* interactions.

3. Biased methods

In the first part of this section we discuss 'biased' methods—that is, schemes for which we build in some pertinent *a priori* information, such as a preferred local coordination or chemical order. We show that judicious inclusion of such information at the start of the simulation can greatly improve the quality of models.

3.1. Molecular dynamics simulation of g-$GeSe_2$ and local building blocks

Molecular dynamics simulation of overconstrained complex glasses at compositions far from stoichiometry is a notoriously difficult problem [17]. For complex glasses, it often happens that the 'cook and quench' technique fails to produce the correct structure. In the absence of *a priori* information, models obtained either contain too many defects or their structures are very poor compared to experiments (for example, incorrect static structure factor $S(Q)$ at large Q). Despite the fact that *ab initio* methods describe the interaction between electrons and ions accurately, such failures can be attributed to unphysical quench rate and inadequate length of simulation time that constrains the system to access the full configuration space. As a result, models obtained from direct MD simulations lack the essential geometrical and topological structure, which are very important in determining the physical properties of the models. One approach to tackle this problem is to use the notion of inferring complex 'building blocks' in the model construction. We illustrate this technique with complex $GeSe_{1.5}$ glass as an example. The idea is based on the following assumptions: the local short-range chemical order does not change drastically between large system and small system; the chemical order of a small cell of a material can be correctly obtained by long *ab initio* MD simulation. One can therefore use accurate *ab initio* MD to produce a small nearly perfect subunit cell, the 'pseudo-crystal', by a very extended annealing for a particular composition. This optimized structure, which includes the appropriate chemical ordering for the given composition (and should also satisfy known experimental information about coordination and chemical order for that glass), may be used to make a larger supercell, which can then be melted and quenched.

We implemented this idea for glassy $GeSe_{1.5}$ as a test case using FIREBALL, a density functional code in the local density approximation (LDA) developed by Sankey and coworkers [18]. This is an approximate *ab initio* local density approach to electronic structure, force and dynamical simulation that was derived from density functional theory using the Harris functional [19] and a minimal basis set. Because the code employs the Harris functional, no self-consistent field iterations are required, which is of great benefit to the code's efficiency. This is a relevant point for glassy materials which require the use of large supercell models [20]. The basis set is minimal (for these systems, one s and three p slightly excited pseudoatomic orbitals per site or 'single zeta' in the language of quantum chemistry). In its original form only weakly ionic systems may be treated; self-consistent versions have been developed recently by Lewis and coworkers [18, 21]. This improved version uses separable pseudopotentials and allows for double-zeta numerical basis sets and polarization orbitals. The calculation

is undertaken entirely in real space which provides substantial computational efficiency. Hamiltonian and overlap matrix elements are precalculated on a numerical grid and the specific values needed for a particular instantaneous conformation are extracted from the tabulated values via interpolation. Naturally, the integral tables need to be generated only once, for a given set of atomic species, rather than performing quadratures 'on the fly' during a MD run. These approximations perform exceptionally well for chalcogenide systems.

We made models of $GeSe_{1.5}$ by randomly placing small numbers of atoms in a cubic supercell according to the desired composition (8 germanium and 12 selenium atoms) with the minimum acceptable distance between atoms of 2 Å. The size of the cubic cell, 8.37 Å, was chosen to make the density of the glass close to the experimental data [22], 0.0341 $Å^{-3}$. The cell was annealed and we obtained a well-thermalized melt at 3500 K. We took three steps to cool the cell. First, the cell was equilibrated to 1436 K for 2.5 ps; then it was slowly cooled to 300 K for approximately 7 ps. In the final step, the cell was steepest-descent-quenched to 0 K and maximum forces smaller in magnitude than 0.02 eV $Å^{-1}$. The final configuration obtained played the role of the 'pseudo-crystal' for the bigger cell. To build a larger supercell we repeated the pseudo-crystal over two periods and obtained a system of 540 atoms. We then melted the large cell at 1500 K for 4 ps, cooled over 300 K for 8 ps and quenched to 0 K. All calculations were performed at constant volume using the Γ point to sample the Brillouin zone to compute total energy and forces.

Figure 1 shows the neutron static structure factor and pair correlation function for $GeSe_{1.5}$ from our simulation along with the experimental data [23] and the results from our 'cook and quench' method. Our calculations show good agreement with experiment. Some points of discrepancy are to be expected for different reasons. The most obvious is the size of our models (540 atoms), which is compared to the thermodynamic limit. In figure 1 we also highlight the differences between experiment, a quench from the melt model and the building blocks model. The FSDP is well reproduced (close in width and centering, and more improved from the melt and quench model in height). Another substantial difference between the quench from the melt and the building blocks models is near 2.5 $Å^{-1}$, at the minimum after the second peak. The first peak in $g(r)$ occurs at a higher r value than for the other compositions (Ge_xSe_{1-x}, $0 \leqslant x \leqslant 0.4$). This can be understood in terms of the disappearance of Ge–Se and Se–Se bonds, and the appearance of additional homopolar Ge–Ge bonds. The composition of $GeSe_{1.5}$ glass is such that, on average, one Ge–Ge bond will be present per Ge site.

In figure 2 we illustrate the partial structure factor and partial pair correlation function for the building block and the cook and quench models. The Ge–Se pairs provide the dominant contribution to the first shell of the pair correlation function with an average bond distance of 2.36 Å. In table 1, we list the averaged bonding distances present in the models and compare them to experiment [23]. Our results are in good agreement with the neutron diffraction measurements.

Where coordination is concerned, we note that, in the building blocks model, about 67.60% of Ge are fourfold-coordinated and 31.48% are threefold-coordinated whereas

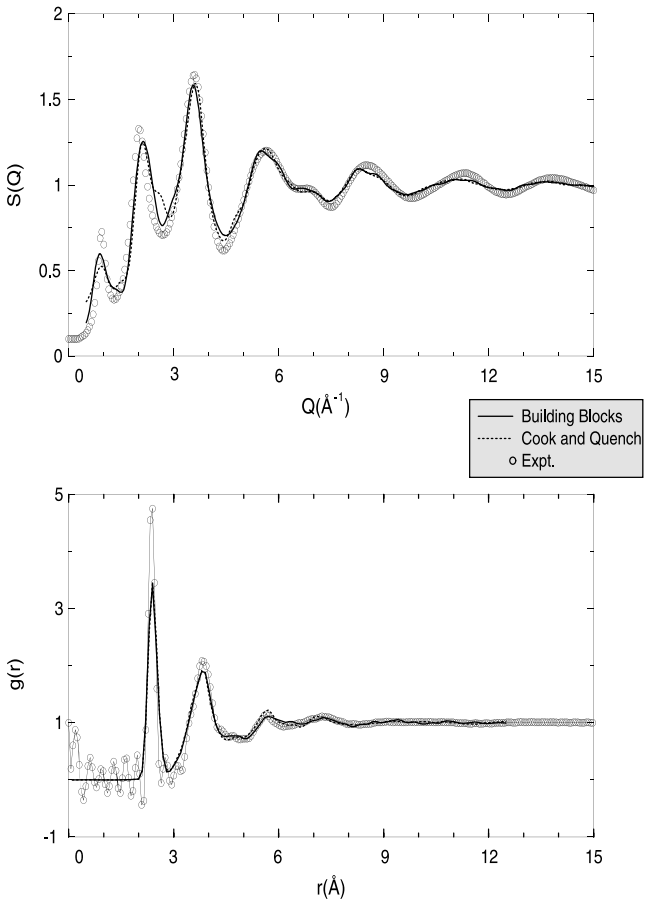

Figure 1. (Top) Neutron-weighted static structure factor, comparing the building blocks model, a 'cook and quench' model with the same Hamiltonian, and experiment [23]. (Bottom) The pair correlation data for the same models along with experimental data as indicated.

Table 1. Average bond lengths in g-$GeSe_{1.5}$ (in Å).

Bond type	Building block	Cook and quench	Petri 2002 [23]
Ge–Ge	2.43	2.44	2.42
Ge–Se	2.36	2.36	2.36
Se–Se	—	2.33	—

67.60% of Se are twofold-, 26.54% are threefold- and 5.56% are onefold-coordinated. The cook and quench model is a different story: about 73.61% and 25.0% of Ge are respectively fourfold- and threefold-coordinated; 60.20%, 30.56% and 9.26% of Se are respectively twofold-, threefold- and onefold-coordinated. We have also noted the presence of fivefold and twofold Ge in the cook and quench model. Where chemical order is concerned, the building blocks model has 93.91% of Ge–Se bonds and 5.43% of Ge–Ge bonds compared to the cook and quench models with 88.38% Ge–Se, 8.88% Ge–Ge and 2.74% Se–Se. The significant amount of Se–Se wrong bonds in the cook and quench model explains the presence of a significant peak in the Se–Se partial pair correlation function. In the building blocks model a negligible fraction is observed. This result is in accordance with the chemically ordered continuous random network model which predicts that, in Ge-rich glasses, Se–Se homopolar bonds are non-existent.

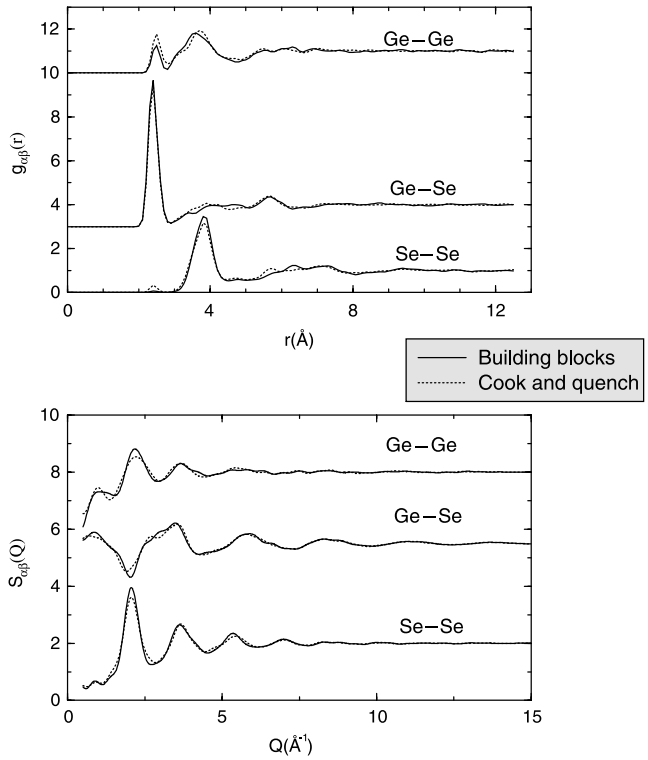

Figure 2. (Top) Partial pair correlation function and partial structure factor, comparing the building block model. (Bottom) Partial structure factors for a 'cook and quench' model of g-$GeSe_{1.5}$.

By integrating the pair correlation function we obtained the average coordination number n. In the building blocks model we found n to be 2.80 compared to 2.81 in the cook and quench model. In EXAFS experiments Zhou *et al* [24] found a coordination number of 2.80 while Petri *et al* obtained a value of 2.81. Our results are consistent with the presence of $Ge_2Se_{6/2}$ ethane-like units in glassy $GeSe_{1.5}$. The electronic density of states of the building blocks model shows a state-free optical gap consistent with experiments [25, 26], of the order of 1.67 eV and the usual limitations of the LDA for predicting the gap.

The notion of inferring building blocks was used by a few authors to model amorphous materials. Ouyang and Ching [27] constructed a model of amorphous Si_3N_4 based on a judicious choice of elementary subunits which satisfy local bonding. The subunits were then connected carefully to meet the bonding requirements of the corner atoms. The randomness was introduced through the random distribution of different subunit types. Although appealing by its simplicity, this approach suffers from long-range crystalline correlations and consequently cannot lead to satisfactory models of amorphous materials [28]. Our method is different from theirs. In our approach the subunit cell, called a 'pseudo-crystal', was built from first principles and the unphysical correlations between the subunit cell were destroyed through the melting process.

Overall the structural properties of the building blocks model are in excellent agreement with experimental data. The discrepancy in the height of the FSDP in $S(Q)$ is probably linked to the model size. There is no evidence that a better Hamiltonian will reproduce the first peak correctly. This pattern has also been observed in $GeSe_4$. In the cook and quench model, the FSDP is less pronounced and the model contains more structural defects.

The approach of inferring building blocks has proven to be successful and can easily be applied to non-stoichiometric and complicated glasses. In their work, Zhang and Drabold [29] made drastically improved models of Ge–As–Se glasses. The models had a state-free optical gap and a satisfactory vibrational spectrum. In contrast a direct quench from the melt approach *with the same total energy functional* starting with the atoms placed randomly in the cell produced highly unrealistic results, for the pair distribution and with far too many electronic defects [30].

3.2. Molecular dynamics simulation via decorate and relax

Decorate and relax (DR) is designed to overcome the limitations of MD, especially the profound limitations of timescales, and for the quench from the melt in particular, the problem of freezing in too much liquid-like character [5]. We have found it to be useful to include primitive *a priori* information about the chemical order and coordination in model construction [29, 31]. This section demonstrates the utility of such an approach for binary glasses. The use of such starting points for *ab initio* modeling puts the simulation in the 'right part' of configuration space (which is of extremely large dimension and complexity). We believe that this 'hunting in the correct subspace' is needed for current simulations with their few several picosecond timescales (with consequent severely limited access to configuration space). There is a pressing need for successful schemes for modeling disordered materials of arbitrary composition.

Using DR, we made models of glasses of composition IV–VI_2. The starting point of the method is a defect-free (fourfold-coordinated) supercell model of column IV (Ge and Si) amorphous materials made with the WWW method [32, 33]. Characteristic of an amorphous column IV material, this model has bond angles tightly centered on the tetrahedral angle, and has a topology presumably unrelated to g-IV–VI_2. The method consists of decorating all the IV–IV bonds with a bond-center VI and rescaling the coordinates to the experimental density of the corresponding glass. The obtained model of g-IV–VI_2 is then quenched to the nearest minimum with an *ab initio* code. The peculiarity of the DR is the presence of a strong, sharp prepeak in the static structure factor of the starting models. This prepeak is very similar to the prominent first sharp diffraction peak (FSDP) feature of glasses. The existence of this peak shows that the starting models already exhibit the intermediate range order associated with the FSDP. In addition, the decorated scheme is much faster than the traditional methods (at least 10 times faster for a given interatomic interaction). To the extent that no scheme can be claimed to mimic the *physical* process of glass formation, this method should be evaluated by its success in reproducing the known experimental information.

The method has been applied to generate several models of binary IV–VI glasses, such as g-$GeSe_2$, g-$SiSe_2$ and g-SiO_2 [5]. The resulting models are in some ways superior to the

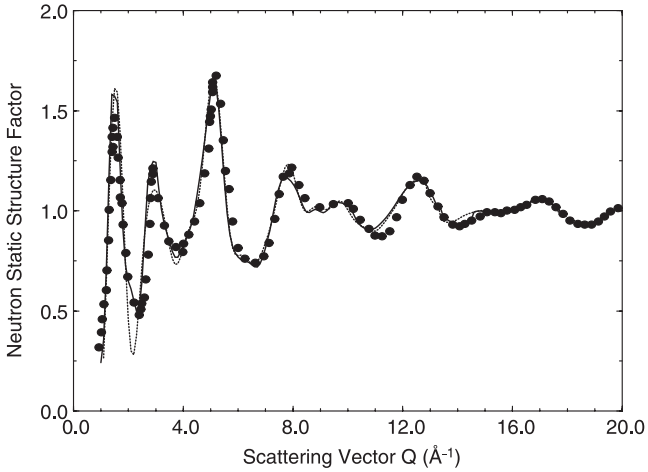

Figure 3. Total neutron static structure factor $S(Q)$ of glassy SiO_2 for the DR models (the dashed line is for the 192-atom model and the solid line is for the 648-atom model) compared to experimental data from [34] (filled circles). The scattering lengths $b_{Si} = 4.149$ and $b_O = 5.803$ fm were used to compute the scattering data.

best models in existence, and are remarkably easy to generate. For example, for g-SiO_2, we have used DR to produce a 648-atom model starting with a defect-free 216-atom model of a-Si. The static structure factor of this model along with experiment and a 192-atom model is illustrated in figure 3, in essentially perfect agreement with experiment [34]. The discrepancy between the 192-and the 648-atom models (especially near 2.0 $Å^{-1}$) arises from finite size effects, since the same Hamiltonian and procedure was used to generate both models. Where chemical order is concerned, the 'decorated' models have 100% heteropolar bonding, as one would expect from the chemistry of silica. Moreover, the models are characterized by the presence of a chemically ordered bond network in which Si-atom-centered tetrahedra are linked by corner-sharing O atoms.

We have also computed the bond angle distribution. In table 2 we compare our results with experiments [35, 36] and theoretical results [37] for the tetrahedral angles O–Si–O and Si–O–Si. The location and the width of the peaks are in good agreement with experimental values. The O–Si–O angle has a mean value of 109.5°, which is near the tetrahedral angle $\Theta_T = 109.47°$, and the full width at half-maximum (FWHM) of the order of 9.0°. On the other hand, the Si–O–Si angle distribution is much broader, with an average value of 140° with an FWHM close to 25°. In their experiment [38], Pettifer *et al* obtained an average value of 142° for the angle Si–O–Si with an FWHM of the order of 26°.

Preliminary work with Chubynsky and Thorpe suggests that the approach may be extended to off-stoichiometry compositions. Such networks have been recently introduced and explored by Chubynsky and Thorpe to study the vibrational excitations of chemically ordered networks [39].

3.3. Unbiased method

It is often unclear where impurities atoms are likely to be found in a disordered network. An ideal example is determining the location of H in a-Si:H. A possible approach is to 'cook and quench' the Si and H atoms in a box with periodic boundary condition (PBC) and a pre-selected density. However, this leads to models electronically much inferior to WWW models of the elemental amorphous material, in clear contradiction with experiment. Fedders and Drabold used 'God's Scissors' to add H to reduce the defect concentration (both dangling bonds and strained bonds) [40]. While the scheme could be justified to some degree by *a posteriori* agreement with experiment, it is very highly biased. In this section, we simply 'release' atomic H into the a-Si network and find that the H selectively attacks strained tetrahedra and coordination defects (in fact, the method is useful for inferring what the chemically reactive locations in the network *are*). We use the same method elsewhere to track Ag^+ dynamics in fast-ion conducting glasses and, in this paper, to directly study polymerization in AsSe glasses.

Table 2. Location and the FWHM (in parentheses) of the angles O–Si–O and Si–O–Si obtained from the simulation and experiments.

	Theory		Experiment	
Angle	Decorate and relax	Vollmayr 1996	Mozzi 1969	Coombs 1985
O–Si–O	109.5° (9°)	108.3° (12.8°)	109.5°	109.7°
Si–O–Si	140° (25°)	152° (35.7°)	144° (38°)	144°; 152°

4. Inverse approach to amorphous materials: a case study of amorphous silicon

In the preceding section we have discussed applications of 'cook and quench' and suitably biased MD in structural modeling of amorphous materials and the remarkable advances they have brought in this field. While direct MD simulations (both first principles and empirical) continue to play a major role in modeling amorphous systems, methods based on inverse approaches have been increasingly used in recent years. It is particularly important to note how inclusion of structural information in the 'decorate and relax' and the 'building block' approaches significantly improves the quality of the models. These are indicative of the fact that the method that can suitably combine or impose useful structural data during the course of simulation may have the advantage of producing more reliable configurations. In contrast to direct methods, inverse methods rely on (1) the availability of useful structural, electronic and spectroscopic data and (2) the effective incorporation of these data into structural modeling of materials. A classical example is reverse Monte Carlo simulation [41]. Unlike the direct molecular dynamics or Monte Carlo simulation, which are based on minimization of an appropriate potential energy functional, the hallmark of the reverse Monte Carlo method is to make use of available experimental data and some known topological properties of the material under study.

McGreevy and Pusztai [41–43] were the first to recognize the potential importance of experimental data, particularly structural, in modeling amorphous materials. A great deal of structural information can be obtained from x-ray and neutron diffraction, and extended x-ray absorption fine

structure (EXAFS) experiments, providing information on pair correlation, coordination and the local bonding environment. A suitable model can therefore be constructed such that the experimental data are built into the model. The central idea is to start with a suitable configuration that satisfies a set of constraints appropriate for the materials under study. Atoms are then displaced randomly using the periodic boundary condition until the input experimental data (such as x-ray diffraction, neutron scattering and extended x-ray absorption) and the constraints match with the data obtained from the generated configuration. This is achieved by minimizing a cost function (via conventional MC) that consists of experimental data as well as some additional material properties in the form of constraints whenever possible. Since the method produces models that include the desired experimental properties in its way of construction, it is inverse in nature and can be used for generating structural configurations to satisfy some selected experimental properties of the materials. The use of additional constraints (which can be both geometrical or topological) restricts the search space, and thereby greatly reduces the unphysical configurations that are mathematically correct solutions. Starting with a system consisting of N numbers of atoms with the periodic boundary condition, one can construct a generalized cost function for an arbitrary configuration:

$$\xi = \sum_{j=1}^{K} \sum_{i=1}^{M} \eta_i^j \{F_E^j(Q_i) - F_c^j(Q_i)\}^2 + \sum_{l=1}^{L} \lambda_l P_l \qquad (1)$$

where η_i^j is related to the uncertainty associated with the determination of experimental data points as well as the relative weight factor for each set of different experimental data. The quantity Q is the appropriate generalized variable associated with experimental data $F(Q)$ and P_l is the penalty function associated with each constraint. For example, in the case of the radial distribution function and structure factor, Q has the dimension of length and inverse length, respectively. In order to avoid the atoms from coming too close to each other, a certain cutoff distance is also imposed, which is typically of the order of interatomic spacing. In RMC modeling, this is usually obtained from the radial distribution function by a Fourier transform of the experimentally measured structure factor. This is equivalent to adding a hard-sphere potential cutoff in the system which prevents the catastrophic build up of potential energy.

Despite the fact that RMC has been applied to many different types of systems [4]—liquid, glasses, polymer and magnetic materials—the reliability of the method is often questionable. This is particularly so in the absence of adequate information (both experimental or otherwise). The method can produce multiple configurations having the same pair correlation function which certainly reduces the utility of the generated structure for further use. This lack of uniqueness, however, is not unexpected in view of the fact that only the pair correlation function or structure factor is used in modeling the structure while there exists an infinite hierarchy of higher-order correlation functions which are not directly accessible from experimental data. In the absence of sufficient information, RMC can only produce the most disordered structure consistent with a given set of experimental data.

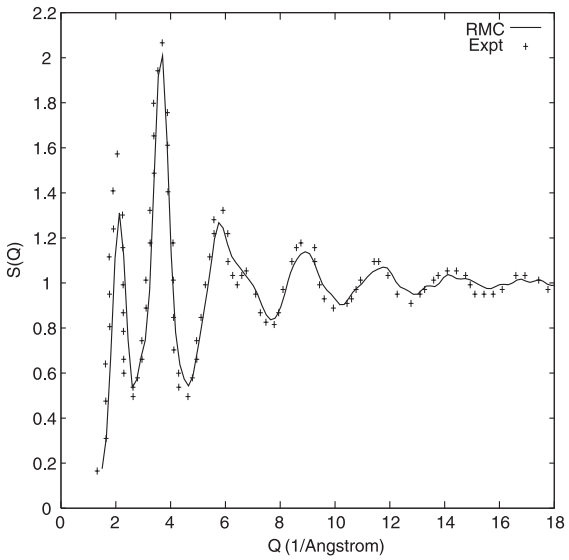

Figure 4. Structure factor of a model configuration obtained from RMC simulation (solid line). The points indicate the experimental data obtained by Laaziri *et al* from [44].

Let us illustrate the method with amorphous silicon (a-Si). This is an archetypal example of amorphous semiconducting system, which is very difficult to build via molecular dynamics simulation. It is neither a glass nor can it be described as a disordered crystalline silicon network owing to its very different topological properties. It has been observed that for realistic modeling one needs to include, at the very least, information about the two-body correlation (via structure factor) and a description of the bonding geometry via average bond angle and its variance. Furthermore, it is also important to include some information about average coordination of the network to describe the tetrahedral bonding. However, the structure factor cannot alone provide such information and consequently RMC fails to generate configurations having *only* the topology of amorphous silicon but a mixture of all those that are consistent with the structure factor or radial distribution function used in the simulation. Metallic glasses, on the other hand, lack directional bonding in the short-range length scale but can have non-trivial intermediate-range structure that may not be possible to obtain in reverse Monte Carlo models unless included explicitly in the model construction. It is therefore essential that for a predictive study RMC models must be verified independently by comparing the electronic, vibrational and optical properties of the model to experimental data whenever possible.

The results for the model amorphous silicon obtained via RMC simulation are presented in figures 4–6. The model is constructed by taking into account pair correlation between the atoms, average bond angle and its deviation, and average coordination number of the atoms. The computed radial distribution is expected to match with the experimental as it was enforced during the simulation. For the bond angle distribution (BAD), we compare the RMC model with a model

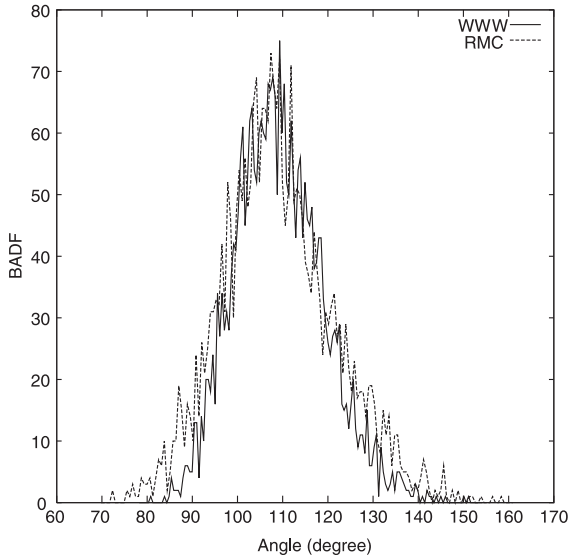

Figure 5. The bond angle distribution for the RMC model (dotted line). The corresponding data from a high quality modified WWW model (see [45]) is also plotted in the figure for comparison. The root mean square deviation of the distributions are 12.3° and 9.5°, respectively.

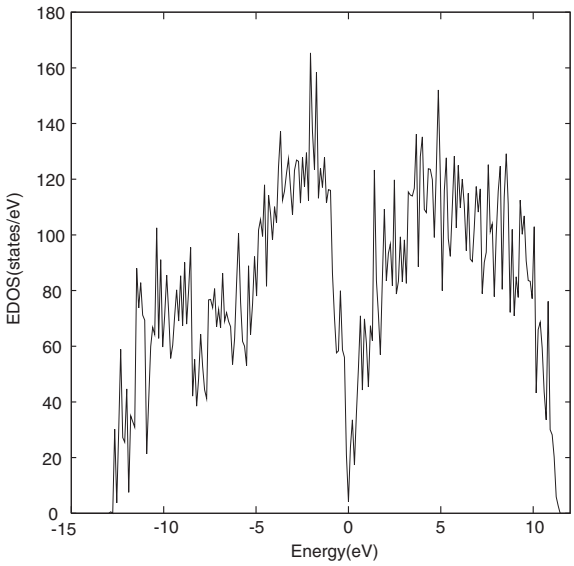

Figure 6. The electronic density of states for the RMC model obtained from a first-principles SIESTA Hamiltonian within the local density approximation as described in the text. The presence of a electronic gap in the spectrum is clearly visible.

obtained from an improved WWW algorithm developed by Barkema and Mousseau [45]. The average bond angle for the RMC model is found to be 109.12° with a root mean square deviation around 12.3°. A more stringent test of the model is look at the electronic and vibrational properties of the model. The electronic density of states (EDOS) obtained from the density functional code SIESTA [46] in the local density approximation (LDA) is plotted in figure 6. The presence of a gap in the spectrum is very noticeable; the gap is, however, not very clean due to the presence of structural defects in the form of dangling bonds. The defects can be minimized by annealing the sample using a suitable force field. The details of the model construction and its properties were studied in [47]. In a similar fashion, one can address other important semiconducting amorphous materials (such as a-C, a-Se and a-SiC) by identifying the right constraints along with sufficient structural data. For multinary systems, one needs to have the partial structure factor for each of the components in addition to relevant constraints to determine the structure unambiguously.

In summary, RMC is a fascinating approach to model amorphous materials provided an adequate set of experimental data is available along with a handful of empirical constraints. The success of the method, however, largely depends on the choice of an optimal experimental dataset so that the resulting optimization problem can be solved without much difficulty. Inclusion of too much information would make the optimization problem very difficult, whereas too little information would cause it to produce too many poor configurations of the material. The identification of an optimal experimental dataset consistent with a set of suitable constraints is of utmost important for RMC modeling. For multinary complex disordered materials, however, a systematic procedure for obtaining optimal information data (both experimental and constraints) is still lacking, and therefore one should be careful in interpreting results of RMC simulation. RMC models should always be verified by studying further experimental properties (that are included in the model construction) before a predictive study of the material can be done. Until the method can be further generalized, it is instructive to study materials case-by-case via RMC, and to compare the same obtained from more traditional approaches.

5. Beyond reverse Monte Carlo: the ECMR method

A closer inspection of the reverse Monte Carlo method described above immediately reveals a major drawback of the method. It is apparent that, for realistic modeling of amorphous materials, one needs to include sufficient information that not only satisfies the input experimental data but also be able to predict correctly the other experimental properties of the materials. This suggests one should enforce *all* the experiments available. This might include structural (x-ray diffraction), electronic (x-ray photo-emission) and vibrational (neutron diffraction) properties for a well-studied material. However, the RMC problem is essentially a non-convex optimization problem and the optimization (of the generalized penalty function) becomes very difficult to solve for increasing number of constraints that might be necessary to produce an acceptable solution. Furthermore, in the absence of any potential energy function, models obtained via RMC may not be in a suitable minimum of the total energy surface and therefore unlikely not to be stable (or metastable) energetically.

The experimentally constrained molecular relaxation or ECMR has been designed to address some of the problems above [48]. Instead of relying on experimental information and a set of constraints only, one attempts to employ additionally an approximate energy functional to describe

the dynamics correctly by merging first-principles density functional (or tight-binding/empirical) as well as experimental data. The purpose of the energy functional is to guide the system *approximately* in the augmented configurational space defined by experimental data and other constraints. The idea is to reduce the number of unphysical configurations that might be mathematically correct but fail to satisfy structural and dynamical behavior correctly. The approximate energy functional constrains the system to evolve on a restricted *but* hypersurface, and thereby accelerates to converge toward realistic solutions during the course of optimization. The configuration obtained from the method is not only a minimum (or local or global) of an appropriate energy functional but is also consistent with the input experimental information:

$$\Xi(\mathbf{Q}, \mathbf{r}) = \xi(\mathbf{Q}) \oplus \gamma E(\mathbf{r}). \tag{2}$$

In equation (2), the symbol $\oplus$ stands for the direct sum of the configuration space of the penalty function $\xi(\mathbf{Q})$ (consisting of experimental data) and that of the energy functional $E(\mathbf{r})$. In the limit γ is infinitesimally small and the method reduces to a inverse method (RMC in the present case), whereas for a very large value of γ the method is equivalent to a direct method of minimizing the total energy.

A possible way to implement this idea is to use minimal experimental information in conjunction with a knowledge of interactions between the atoms. For complex materials, however, such identification of 'minimal' constraints is a non-trivial task, and to a large extent depends on the relative hierarchy of the constraints used in the simulation. A simple approach to improve the method is to add a constraint in RMC (an additional P_l in ξ in equation (2)) to minimize the magnitude of the force on all the atoms according to some energy functional or possibly to minimize the total energy/force. Such an approach is expensive, particularly for *ab initio* Hamiltonians, since Monte Carlo minimization of equation (2) requires a large number of energy/force evaluations. To reduce the computational burden, one may therefore employ a simple iterative scheme consisting of the following steps: (1) starting with an initial 'generic' configuration C_1, minimize ξ to get C_2, (2) total energy minimization of C_2 via an *ab initio* method to get C_3, (3) subject the resulting configuration to another optimization via RMC (minimize ξ again), then repeat steps (2) and (3) until both the force-field relaxed model and RMC models no longer change with further iterations. For the RMC component of the iteration, conventional Monte Carlo minimization is used but other methods such as those based on quasi-Newton techniques can be used as well.

A schematic representation of the various steps is shown in figure 7. At the heart of the method lies two self-consistent loops that are connected with each other to navigate the system along the multi-dimensional configuration space. The evolution of the system is then tracked by introducing two convergence parameters (χ_{rmc} and χ_{fp}) for minimization and first-principles relaxation. The parameters dynamically correct the system to propel along the right part of the augmented solution space that is both optimally satisfied total energy and force, and the deviation from the experimental

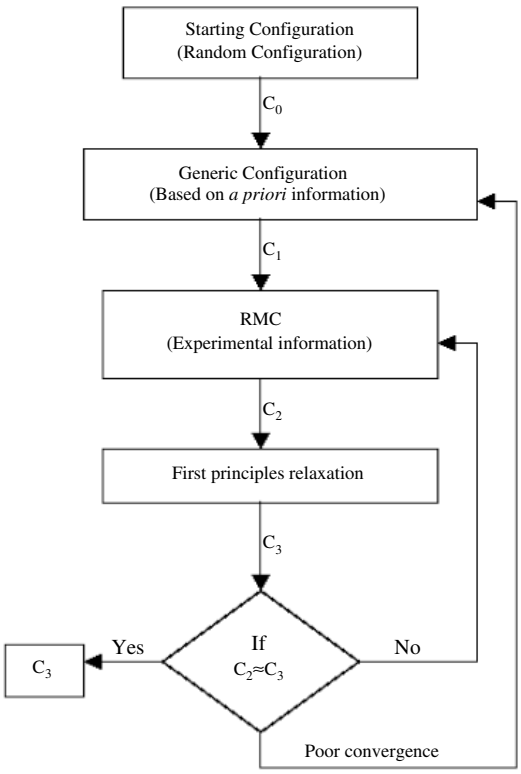

Figure 7. A schematic representation of the ECMR method. Starting from a generic configuration, the method self-consistently minimizes the total energy and experimental constraints until an optimum convergence is achieved.

data. By appropriately choosing a generic configuration, the convergence of each part can be accelerated by the other. In the event convergence is not achieved within the specified iterations, the method automatically generates a new configuration using a different set of information. Details of the method can be found in [48]. Since the method directly uses experimental information in association with total energy relaxation (either first principles or otherwise), we refer to this method as experimentally constrained molecular relaxation (ECMR).

ECMR has been applied recently to amorphous $GeSe_2$ and hydrogenated amorphous Si [48, 52]. The former is a classic glass former and has interesting physical properties that are difficult to model via conventional molecular dynamics simulation [49, 50]. A characteristic feature of $GeSe_2$ is the presence of strong intermediate-range order that results in a first sharp diffraction peak (FSDP) observed in neutron diffraction measurements. Models obtained from MD simulation usually show none or a very weak presence of the FSDP that is not compatible with experimental data. The intermediate-range order in this material is generally attributed to the presence of tetrahedral motifs having edge- and corner-sharing topology. Raman spectroscopy and neutron diffraction provide useful information about the topological structure of the material [53, 54]. The $GeSe_2$ model simulated via the ECMR method has been discussed at length in a recent communication by the authors [48]. Here we briefly mention some of the salient features of the model starting with the

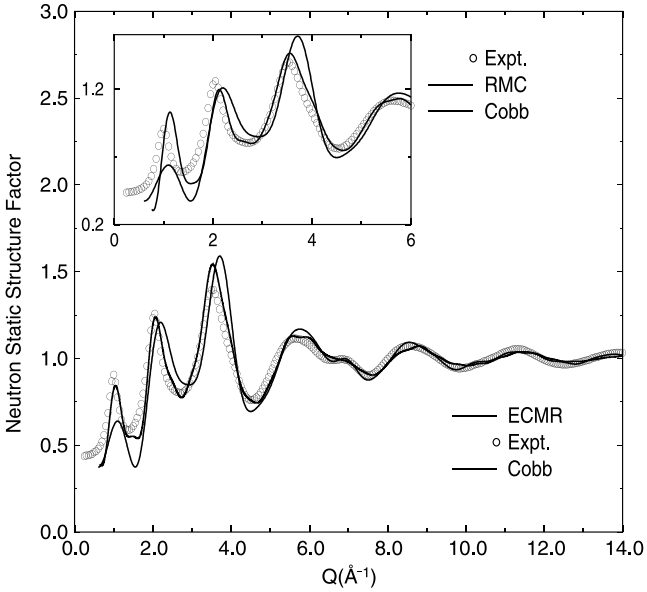

Figure 8. Neutron-weighted static structure factor for two different models obtained from ECMR and molecular dynamics simulation ([49] and [50]). The experimental data are taken from [51]. The result from the RMC is also plotted in the inset.

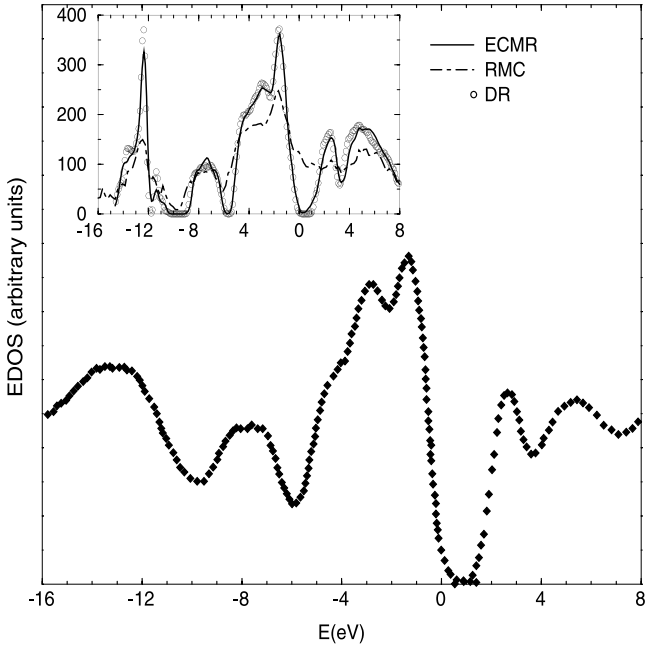

Figure 9. The electronic density of states (EDOS) of the ECMR, DR and RMC models of glassy $GeSe_2$ (in the inset). The x-ray (XPS) and inverse photo-emission (IPES) data show the valence and conduction band of the spectrum, respectively, with the Fermi level located at $E = 0$ eV. Note the absence of a gap in the RMC model.

static structure factor. The neutron-weighted static structure factor obtained from the ECMR model is plotted in figure 8 along with the experimental data from Petri *et al* [51] and the data obtained by Cobb *et al* in [49]. The computed data from the ECMR model fits very well with the experimental data. The network topology of g-$GeSe_2$ is also studied and is found to be correctly produced via ECMR. Raman spectroscopy and neutron diffraction measurements [53, 54] indicated that about 33%–40% of Ge atoms are involved in forming edge-sharing tetrahedra. An examination of the ECMR model reveals the corresponding percentage is about 38%. This is remarkable in view of the fact that such information is not included in the initial configuration. This observation indeed suggests that imposition of partial pair correlation functions and first-principles relaxation via ECMR does produce a model having better topological properties than MD or RMC can do alone. The network topology can be further characterized by looking at the partial coordination numbers (nearest neighbor) providing information on the plurality of the local bonding environment. The values for Ge–Ge, Ge–Se and Se–Se obtained from the ECMR model are 0.17, 0.30 and 3.68 compared to experimental values (from partial structure factors) 0.25, 0.20 and 3.7, respectively. As a further check of the reliability of the ECMR model of a-$GeSe_2$, the electronic density of states are calculated to compare with experimental data obtained from x-ray photo-emission (XPS). The electronic density of states of the ECMR model (shown in the inset) is in good agreement with the x-ray photo-emission (XPS) [25] and inverse photo-emission spectroscopy (IPES) [26], and establishes further the credibility of our method. The electronic density of states for the ECMR, RMC and DR models along with the experimental data are plotted in figure 9.

6. Vulcanization in amorphous materials: applications to As–Se glass

Some amorphous materials, such as amorphous Se, containing long 1D chain structures can be described as polymeric glasses because of their similarity in the network structure with real polymers. Of particular interest is the formation of complex polymer-like structures these materials exhibit in the presence of some elemental species (As, for example). Inclusion of such species can cause the original chain structure to evolve into a complex 3D random network [55, 56]. This process is often termed as 'vulcanization' in amorphous science. An example of such a system is As–Se glass at a low concentration of As. Computational modeling of such systems are of special interest as it provides an opportunity to study the 'polymerization' behavior in real glasses and the corresponding change in the structural properties of the network.

In this section, we briefly mention our approach to study 'vulcanization' via first-principles molecular dynamics simulation. Starting with a 64-atom a-Se model, As atoms were introduced in a controlled manner to study the formation of such polymer-like chains as the simulation proceeded. For our purpose, we employed some special strategies during the course of simulation. Since modeling a-Se itself is a non-trivial work, we began with a relatively small model of a-Se developed by one of us [29]. This initial configuration satisfied both structural and electronic properties of a-Se and had very low structural defects. Since we are primarily interested here in the 'polymerization' process only via formation of special vulcanized units, we constrained ourselves to a small but high quality model of a-Se only. Arsenic atoms were

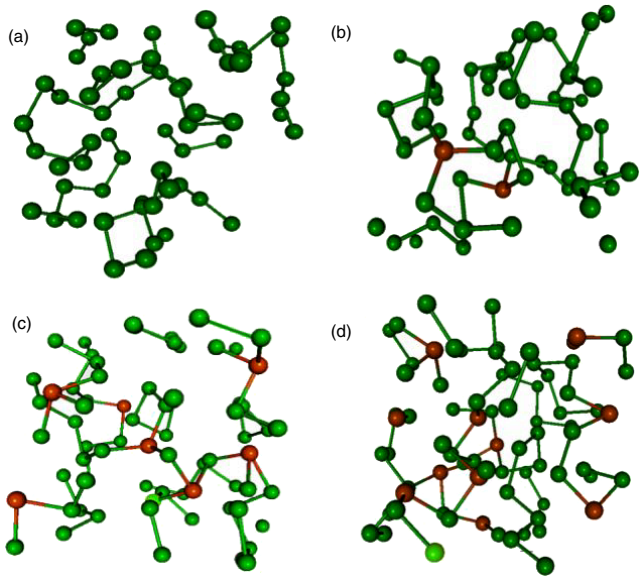

Figure 10. (Color online only) Formation of amorphous As–Se networks at three different concentrations: (a) the initial 64-atom glassy Se (green) network, (b) Se network with 3% of As (red) atoms, (c) Se network with 10% of As (red) and (d) Se network with 15% As (red) atoms. The presence of As–Se–As cross-links are clearly visible in (d).

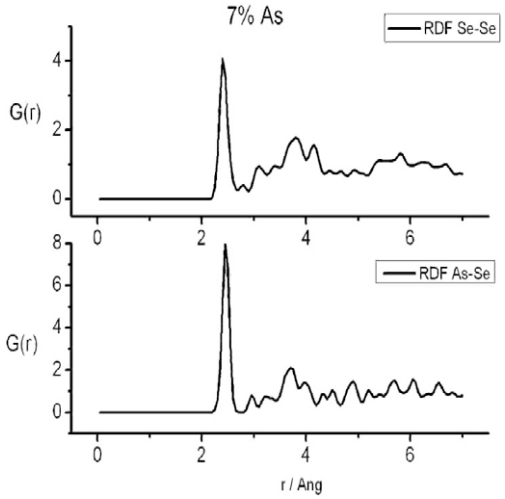

Figure 11. The partial radial distributions for As–Se and Se–Se at 7% As concentration.

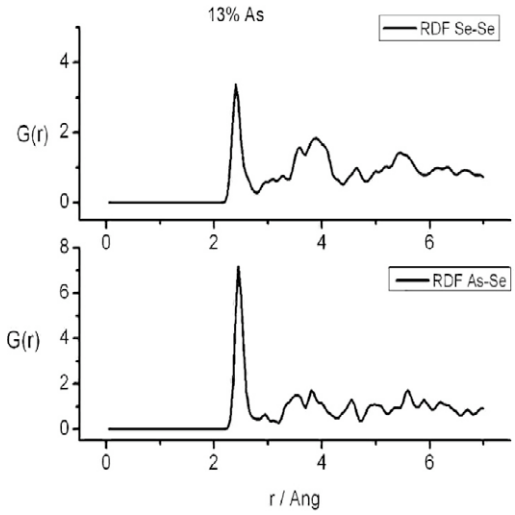

Figure 12. The partial radial distributions for As–Se and Se–Se at 13% As concentration. The height of the first Se–Se peak has reduced (compared to that of 7%) due to As–Se–As structure formation.

introduced into the a-Se network at random initial positions subject to the condition that they were not far away from the Se chains. The MD simulation then proceeded by using a plane wave basis set for expanding eigenfunctions and the ultrasoft Vanderbilt pseudopotential as implemented in the Vienna *ab initio* simulation package (VASP) [57]. The system was equilibrated at 300 K using the NVT ensemble.

The results from our simulation are presented in the figures 10–12. In figure 10, we have shown the formation of stable vulcanized units at three different concentrations—5%, 10% and 15%. It is clear from the figure that, with increasing concentration, more and more non-bonded As atoms connected to the network and formed 3D-like structures. Selenium chains were broken and cross-linking units of As–Se were formed until the long chains were tightly connected together. It is apparent from the figure that at 15% there is significant change in the original structure, particularly via formation of 'As–Se–As' triplets. One can expect that at higher concentrations such changes might be more prominent and would cause the 1D chain structure to evolve into a complex 3D continuous network. This might lead to the formation of new structural units and possibly phase transitions. These units form the vulcanized units that cross-link between As and Se atoms. The radial distributions of the resulting As–Se glass at concentrations 7% and 13% of As atoms are plotted in figures 11 and 12, respectively. The partial pair correlation functions for the As–Se system obtained by this method appear very good.

In figure 13 we have shown the formation of cross-linking structure. A possible reason for the formation of cross-links would be as follows: the Se chains in the network are very flexible; they can twist and fluctuate while bonded to the rest of the network. When As atoms move close to Se chains, the system prefers to form Se–As bonding to minimize the total energy, and thereby provides a route to cross-link As atoms to Se chains. The cross-linking makes the resulting Se chain containing As–Se–As triplets more stable. The process continues until the Se chains evolve into a more complex 3D random network.

This method is particularly suitable at low concentrations of As atoms, and when high quality models of Se are readily available. In order to avoid the formation of As clusters, As atoms were introduced close to Se chains and relatively far away from other As atoms. At high concentration, however, care must be taken to introduce As atoms step-by-step so that atoms can get plenty of time to form a network with the Se chains.

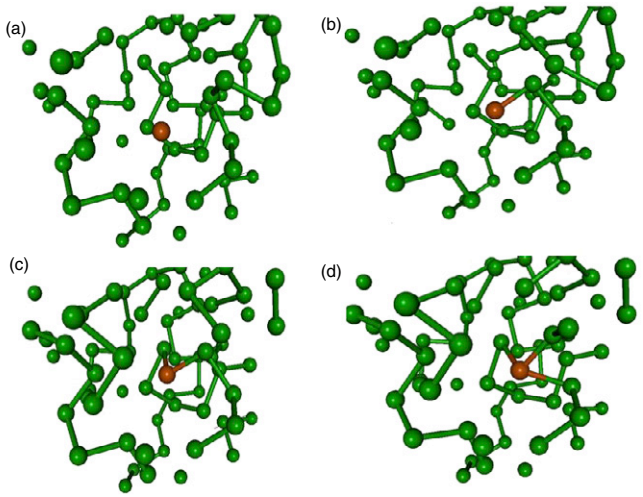

Figure 13. (Color online only) The various steps in cross-link formation between As (red) and Se (green) atoms. (a) A non-bonded As atom in the network, (b) the first bond formation with a neighboring Se atom in a 1D chain, (c) second bond formation and (d) the completion of cross-link formation for the As atom in the network.

7. Hydrogen distribution in amorphous silicon: a first-principles study

Hydrogenated amorphous silicon (a-Si:H) is a very important material with a wide variety of technological applications. Since its first preparation in the late 1960s, the application of a-Si:H ranges from photovoltaics to memory switching devices, thin film transistors, solar cells, optical scanners and numerous other electronic instruments [58]. Experimentally, it is still one of the most active fields of research in materials science that continues to produce a large volume of experimental information. In spite of this, our understanding of the role of H in a-Si:H from a theoretical point of view is very limited. Some of the very fundamental processes involving the material are poorly understood. The creation of metastable defects in the material upon prolonged exposure to light, the so-called Staebler–Wronski effect [59], is perhaps the most intriguing problem in this field that is directly related to H microstructure in a-Si:H. Nuclear magnetic resonance (NMR) studies have clearly revealed that H distribution in a-Si:H can be rather inhomogeneous. A narrow line in the typical NMR spectrum of a-Si:H signifies the presence of Si–H monohydride along with a broad line that is generally attributed to clusters of Si–H in the network. Furthermore, multiple-quantum NMR experiments suggest that the typical number of H atoms in a cluster is about 5–7 in device-quality a-Si:H. Theoretical efforts to understand the microscopic origin of NMR linewidths are very limited in spite of the impressive development of new models in recent years. There exists a number of important studies on modeling a-Si:H that mostly focus on structural and electronic aspects of the material properties. The methods employed to obtain these models can be broadly divided into two categories: dynamic and static. As discussed earlier, the dynamic 'cook and quench' method consists of direct MD simulation by melting crystalline Si with H at high temperature and then quenching the system from the melting point to room temperature in several steps to arrive at the amorphous phase [60–62]. For a-Si:H, the method naturally produces too many topological defects (such as dangling and floating bonds, and liquid-like local structure) with poor electronic and optical properties. The static approach involves adding H selectively in the network at some strained Si sites, and to relaxing and passivating the network to reduce the defect density [63, 64, 52]. While the latter can produce a good quality a-Si:H model with low defect density and correct structural and electronic properties, it is not yet clear to what extent H microstructure can be correctly described within this approach. A device-quality model of a-Si:H must satisfy not only structural, electronic and vibrational experiments but also conform to NMR studies to take into account correct H dynamics and its distribution in the network.

In the following we present a first-principles study of modeling hydrogenated amorphous silicon, with particular emphasis on the distribution of H atoms in the network. To this end, we started with a 216-atom model of an a-Si network and introduced 24 H atoms randomly at a distance of about 2.5 Å from the host Si atoms. This amounts to having approximately 10% of H in the network by number or about 1% by atomic weight. Such a low concentration of hydrogenated sample can be grown experimentally by hot wire chemical vapor deposition (HW-CVD) [65]. This initial configuration was then equilibrated using NVT simulation at $T = 300$ K for about 4 ps using the first-principles density functional code VASP [57]. The resulting network reorganized itself and the H atoms formed bonds with the host Si atoms. The H atoms were found to be particularly reactive in the vicinity of strained Si–Si bonds in the network. Strained Si–Si bonds were broken and new Si–H bonds were formed. This process reduced the strain of the network and passivated any dangling bonds that might have been created during the equilibration process. The movement of the H atoms was tracked during the simulation, and the nearest-neighbor H–H distances were noted for the last 0.3 ps of the simulation in order to get an idea of H distribution in the network.

In figure 14 we plotted the distribution of minimum H–H distances averaged over a time period of 0.3 ps. The first peak around 2.4 Å is consistent with the average H–H distance extracted from the analysis of proton NMR-free induction-decay (FID) signal reported by Hansen *et al* in [66]. While direct comparison with experimental data is difficult, one can nevertheless calculate the approximate NMR linewidth for the sample (as full width at half-maximum (FWHM)) from a knowledge of the hydrogen distribution in the network. By assuming that the lineshape is Gaussian (which is consistent with experiment at *low* concentrations of H), and is broadened by ^{1}H homonuclear dipolar interactions, the linewidth can be expressed as [67]

$$\sigma\,(\mathrm{kHz}) = 190\left(\frac{1}{N}\sum_{i,j=1}^{N}\frac{1}{r_{ij}^6}\right)^{1/2} \qquad (3)$$

where N is the number of spins (H nuclei) and r_{ij} is the distance between the spins in Å. At 300 K, we observed σ varied between 15 and 20 kHz which was close to the

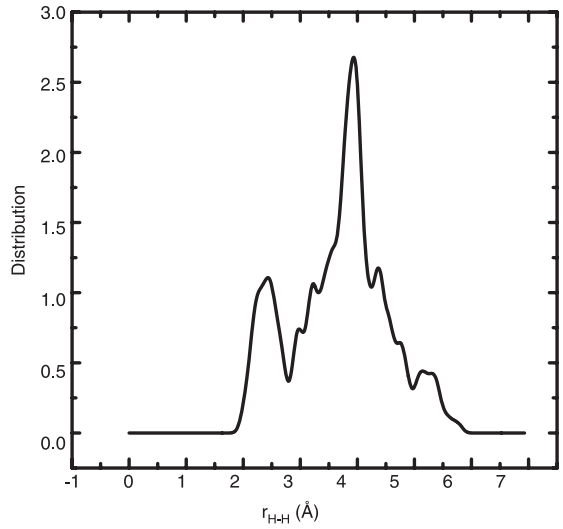

Figure 14. Distribution of minimum H–H distances in amorphous Si216H24 model averaged over 0.30 ps at $T = 300$ K.

experimental range of 22–35 kHz for device-quality a-Si:H samples [68, 69]. The percentage of clustered H configuration was found to be quite small and was about 20% of the total H content. This small number of clustered H is probably due to the short equilibration time and the lower topological defects present in the a-Si network as clustering is most likely to occur around vacancies or voids. Nevertheless, such a configuration is comparable to the device-quality samples grown with a glow discharge (GD) technique which shows the FWHM for a broad NMR line below 35 kHz and average spin concentration for dilute H as 1.5×10^{21} cm^{-3} compared to 4.2×10^{21} cm^{-3} in our model [67]. As H configuration in the a-Si network is largely affected by the preparation conditions (deposition rates, growth temperatures, etc), it is possible that with this improved technique one can get a wide range of H configurations by equilibrating the cell at different temperatures. This is the first time, using *ab initio* simulation, H distribution in a-Si is obtained which is consistent with both the broad and narrow NMR lines.

Acknowledgments

PB acknowledges the support of the University of Southern Mississippi under grant no. DE00945. DAD thanks the NSF for support under grant nos. DMR 0605890 and 0600073, and the ARO under grant no. MURI W911-NF-06-2-2006.

References

[1] Boolchand P, Georgiev D G and Goodman B 2001 *J. Optoelectron. Adv. Mater.* **3** 703
[2] Drabold D A, Biswas P, Tafen D and Atta-Fynn R 2004 Recent developments in computer modeling of amorphous materials *Non-Crystalline Materials for Optoelectronics* vol 441, ed G Lucovsky and M Popescu (Bucharest: INOE)
[3] Drabold D A 2002 *Curr. Opin. Solid State Mater. Sci.* **5** 509
[4] McGreevy R L 2001 *J. Phys.: Condens. Matter* **13** R877
[5] Tafen D N and Drabold D A 2003 *Phys. Rev.* B **68** 165208
[6] Cappelletti R L, Cobb M, Drabold D A and Kamitakahara W A 1995 *Phys. Rev.* B **52** 9133
Zhang X and Drabold D A 2000 *Phys. Rev.* B **62** 15695
[7] Fabricius G, Artacho E, Sanchez-Portal D, Ordejon P, Drabold D A and Soler J M 1999 *Phys. Rev.* B **60** R16283
[8] Tafen D N, Drabold D A and Mitkova M 2005 *Phys. Rev.* B **72** 054206
[9] Blundell T L and Johnson L N 1976 *Protein Crystallography* (New York: Academic)
[10] Jaynes E T 2003 *Probability Theory: the Logic of Science* (Cambridge: Cambridge University Press)
[11] Balasubramanian S and Rao K J 1993 *J. Phys. Chem.* **97** 8835
[12] Karthikeyan A and Rao K J 1997 *J. Phys. Chem.* **101** 3105
[13] Simmons C J, Ochoa R and Neidt T M 1993 *Experimental Techniques in Glass Sciences* ed C J Simmons and O H El-Bayomi (Westerville, OH: The American Ceramic Society) p 315
[14] Kob W 1999 *J. Phys.: Condens. Matter* **11** R85–115
[15] Martin R M 2004 *Electronic Structure: Basic Theory and Practical Methods* (Cambridge: Cambridge University Press)
[16] Finnis M 2003 *Interatomic Forces in Condensed Matter* (Oxford: Oxford University Press)
[17] Thorpe M F, Jacobs D J, Chubynsky M V and Phillips J C 2000 *J. Non-Cryst. Solids* **266–269** 872
[18] Sankey O F and Niklewski D J 1989 *Phys. Rev.* B **40** 3979
Sankey O F, Drabold D A and Adams G B 1991 *Bull. Am. Phys. Soc.* **36** 924
[19] Harris J 1985 *Phys. Rev.* B **31** 1770
[20] Drabold D A 2000 *Insulating and Semiconducting Glasses* ed P Boolchand (Singapore: World Scientific) pp 607–52
[21] Lewis J P, Glaesman K R, Voth G A, Fritsch J, Demkov A A, Ortega J and Sankey O F 2001 *Phys. Rev.* B **64** 195103
[22] Borisova Z U 1981 *Glassy Semiconductors* (New York: Plenum)
[23] Petri I and Salmon P S 2002 *Phys. Chem. Glasses* C **43** 185
[24] Zhou W, Pasesler M and Sayers D E 1991 *Phys. Rev.* B **43** 2315
[25] Bergignat E, Hollinger G, Chermette H and Pertosa P 1988 *Phys. Rev.* B **37** 4506
[26] Hosokawa S, Hari Y, Ono I, Nishihara K, Taniguchi M, Matsuda O and Murase K 1994 *J. Phys.: Condens. Matter* **6** L207
[27] Ouyang L and Ching W Y 1996 *Phys. Rev.* B **54** R15594
[28] Mousseau N 1997 *Phys. Rev.* B **56** 14190
[29] Zhang X and Drabold D A 1999 *Phys. Rev. Lett.* **83** 5042
Zhang X and Drabold D A 2003 *Phys. Rev. Lett.* **83** 165208
Tafen D N and Drabold D A 2005 *Phys. Rev.* B **71** 054206
[30] Zhang X 2001 *PhD Thesis* Ohio University
[31] Drabold D A and Li Jun 2001 *Curr. Opin. Solid State Mater. Sci.* **5** 509
[32] Wooten F and Weaire D 1987 *Modeling Tetrahedrally Bonded Random Networks by Computer* (*Solid State Physics*) ed H Ehrenreich, D Turnbull and F Seitz (New York: Academic) p 40
[33] Mousseau N 2004 private communication
[34] Johnson P A V, Wright A C and Sinclair R N 1983 *J. Non-Cryst. Solids* **58** 109
[35] Mozzi R L and Warren B E 1969 *J. Appl. Crystallogr.* **2** 164
[36] Coombs P G, De Natale J F, Hood P J, McElfresh E K, Wortman R S and Schackelford J F 1985 *Phil. Mag.* **51** L39
[37] Vollmayr K, Kob W and Binder K 1996 *Phys. Rev.* B **54** 15808
[38] Pettifer R F, Dupree R, Farnan I and Sternberg U 1988 *J. Non-Cryst. Solids* **106** 408
[39] Chubynsky M and Thorpe M F 2002 *Physics and Applications of Disordered Materials* ed M Popescu (Bucharest: INOE) p 229
[40] Fedders P A and Drabold D A 1993 *Phys. Rev.* B **47** 13277
[41] Keen D A and McGreevy R L 1990 *Nature* **344** 423
[42] Gereben O and Pusztai L 1994 *Phys. Rev.* B **50** 14136
[43] Walters J K and Newport R J 1996 *Phys. Rev.* B **53** 2405
[44] Laaziri K, Kycia S, Roorda S, Chicoine M, Robertson J L, Wang J and Moss S C 1999 *Phys. Rev. Lett.* **82** 3460

[45] Barkema G T and Mousseau N 2000 *Phys. Rev.* B **62** 4985
[46] Ordejón P, Artacho E and Soler J M 1996 *Phys. Rev.* B **53** R10441
[47] Biswas P, Atta-Fyn R and Drabold D A 2004 *Phys. Rev.* B **69** 195207
[48] Biswas P, Tafen D N and Drabold D A 2005 *Phys. Rev.* B **71** 054204
[49] Cobb M, Drabold D A and Cappelletti R L 1996 *Phys. Rev.* B **54** 12162
[50] Zhang X and Drabold D A 2000 *Phys. Rev.* B **62** 15695
[51] Petri I, Salmon P S and Fische H E 2000 *Phys. Rev. Lett.* **84** 2413
[52] Biswas P, Atta-Fynn R and Drabold D A 2007 *Phys. Rev.* B **76** 125210
[53] Jackson K, Briley A, Grossman S, Porezag D V and Pederson M R 1999 *Phys. Rev.* B **60** R14985
[54] Susman S, Volin K J, Montague D G and Price D L 1990 *J. Non-Cryst. Solids* **125** 168
[55] Mikla V I 2008 *J. Optoelectron. Adv. Mater.* **10** 138
[56] Golovchak R, Kovalskiy A, Miller A C, Jain H and Shpotyuk O 2007 *Phys. Rev.* B **76** 125208
[57] Kresse G and Furthmuller J 1996 *J. Comput. Mater. Sci.* **6** 15
Kresse G and Furthmuller J 1996 *Phys. Rev.* B **54** 11169
[58] Street R A 1991 *Hydrogenated Amorphous Silicon* (Cambridge: Cambridge University Press)
[59] Staebler D and Wronski C R 1977 *Appl. Phys. Lett.* **31** 292
[60] Drabold D A, Fedders P A, Klemm S and Sankey O F 1991 *Phys. Rev. Lett.* **67** 2179
[61] Buda F, Chiarotti G L, Car R and Parrinello M 1999 *Phys. Rev.* B **44** 5908
[62] Klein P, Urbassek H M and Frauenheim T 1999 *Phys. Rev.* B **60** 5478
[63] Holender J M, Morgan G J and Jones R 1993 *Phys. Rev.* B **47** 3991
[64] Tuttle B and Adams J B 1996 *Phys. Rev.* B **53** 16265
[65] Mahan A J, Carapella J, Nelson B P, Crandall R S and Balberg I 1991 *J. Appl. Phys.* **69** 6728
[66] Hansen E W, Kjekhus A and Odden J O 2007 *J. Non-Cryst. Solids* **353** 2734
[67] Wu Y, Stephen J T, Han D X, Rutland J M, Crandall R S and Mahan A H 1996 *Phys. Rev. Lett.* **77** 2049
[68] Baum J, Gleason K K, Pines A, Garroway A N and Reimer J A 1986 *Phys. Rev. Lett.* **56** 1377
[69] Gleason K K, Petrich M A and Reimer J A 1987 *Phys. Rev.* B **36** 3259